Numerical Investigation of Assisted Initiation of Oblique Detonation Waves by Energy Deposition

Ziqi Jiang[1], Zijian Zhang[2], Zongnan Chen[3], Jiaao Hao[1], Chih-yung Wen[1]
[1]Department of Aeronautical and Aviation Engineering, The Hong Kong Polytechnic University, Hong Kong S.A.R, China
[2]School of Aerospace Engineering, Beijing Institute of Technology, Beijing, China
[3]School of Aerospace Engineering, Beijing Institute of Technology (Zhuhai), Zhuhai, China

1 Introduction

Detonation initiation emerges as a prerequisite for the stable operation of an oblique detonation engine (ODE), garnering substantial attention from scholars. For the initiation of oblique detonation waves (ODWs) to happen, a necessary length is required, which exhibits a strong dependence on inflow parameters [1]. It can be elongated by orders of magnitude under challenging flight conditions characterized by low Mach number and high altitudes, exceeding the length of the ODE combustor and precipitating initiation failure or combustion extinction, finally resulting in the unstart of the ODE [2], [3].

Various initiation-assistance methods have been proposed to expand the flight envelope of ODEs, which can be broadly categorized into passive and active initiation methods. Among them, plasma-based methods, as one type of various active initiation methods, have emerged as promising candidates for ignition assistance and combustion enhancement in supersonic flows [4], primarily manifesting through thermal effects for conventional plasma actuators [5]. While extensive research has addressed the effectiveness of plasma-based initiation methods for supersonic combustible mixtures, the application to ODW initiation remains largely unexplored, particularly regarding thermal effects.

This study aims to investigate the thermal effect of plasma-assisted initiation of wedge-induced ODWs with special emphasis on the impact of amounts of energy and forms (continuous and pulsatile) of energy deposition on the ODW initiation characteristics. The spatiotemporal evolution characteristics of the ODW initiation assisted by pulsatile energy deposition are revealed by wave structures analysis in the initiation process. The investigation aims to provide insights into practical applications of plasma-assisted initiation in ODEs.

2 Methodology

Plasma-assisted initiation of ODWs is investigated by utilizing a finite wedge in hypersonic combustible flow, as illustrated in Figure 1(a). The physical model consists of a finite wedge with an inclined angle of 20° and a wedge length L_w = 60 mm, followed by which is an expansion corner of 20° as well. The

Correspondence to: zjzhanglw@gmail.com (Z. Zhang)

solid wall after the expansion corner is parallel to the inflow direction. The inflow is well-premixed stoichiometric H_2/air mixtures at Mach number Ma = 7, static temperature T_0 = 300 K, and static pressure p_0 = 50 kPa. As such inflow interacts with the wedge, it generates only an oblique shock wave (OSW) without inducing any combustion on the finite wedge.

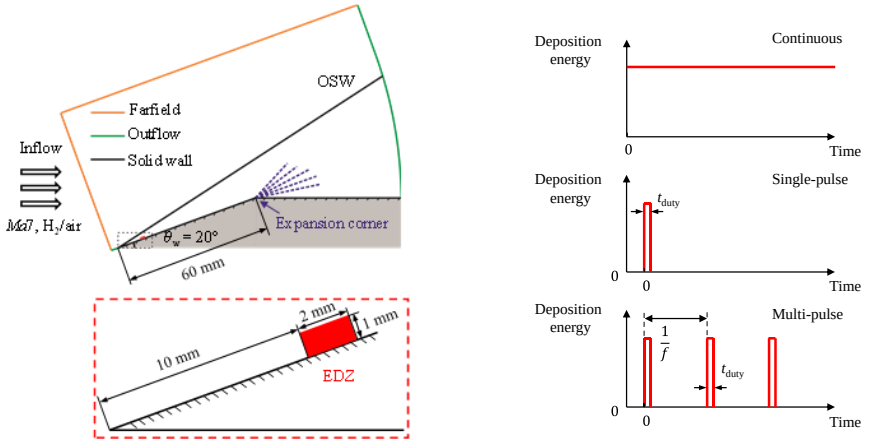

(a) (b)

Figure 1: Schematics of (a) a 20° finite wedge placed at a Mach 7 inflow of stoichiometric H_2/air mixture with a zoomed-in view near the wedge tip and (b) different deposition schemes within the EDZ.

To examine the thermal effect of plasma actuators on ODW initiation, a small rectangular energy deposition zone (EDZ) with dimensions of 2 mm (width) × 1 mm (height) is placed 10 mm downstream from the wedge tip, introducing a homogenous gas heating effect within the EDZ. In alignment with two different forms of plasma actuators (continuous and pulsatile), different energy deposition schemes are implemented, namely continuous, single-pulse, and multi-pulse energy deposition schemes, as shown in the schematics in Figure 1(b). In the continuous energy deposition scheme, EDZ is constantly turned on, maintaining a certain amount of deposition power throughout the entire process, as shown in the upper schematic of Figure 1(b). In a single-pulse energy deposition scheme, the EDZ was first turned on for a limited duty time t_{duty} and remained off for the rest of the process. In the multi-pulse energy deposition scheme, the EDZ was turned on at a certain pulsatile repetition frequency f, forming a cycle duration of $1/f$. The duty time within each cycle is t_{duty}. In this study, t_{duty} = 100 ns was used for all pulsatile energy depositions. f = 50 kHz was utilized for multi-pulse energy deposition.

The ODW initiation over the finite wedge with energy deposition is governed by the two-dimensional (2-D) multispecies reactive Reynolds-averaged Navier-Stokes (RANS) equation. The compressibility-modified Spalart-Allmaras (S-A) turbulence model proposed by Edwards and Chandra [6] is implemented. Chemical kinetics are modeled via a 9-component, 19-step elementary reaction model initially proposed by Jachimowski [7] and modified by Wilson & MacCormack [8]. Energy deposition within the EDZ is realized through source term implementation in the energy equation. The governing equation is numerically solved by an in-house Finite Volume Methods-based solver named PHAROS [9 − 11]. The inviscid fluxes are calculated utilizing the modified Steger-Warming scheme, and the second-order MUSCL with van Leer Limiter is utilized for reconstruction [12]. The viscous fluxes are calculated through a second-order central difference scheme. A method of second-order implicit point relaxation is employed for time-accurate simulations.

3 Results and Discussions

3.1 Continuous Energy Deposition

Through continuously depositing energy within the EDZ, three distinct initiation modes are observed with progressive elevation of deposition power P_{in}, namely, Failed Initiation, Delayed Initiation Mode,

and Direct Initiation Mode. The comparison between initiation modes under the continuous energy deposition is shown in Figure 2. When P_{in} = 12 kW/cm, insufficient energy deposition could not induce combustion, only to create a high-temperature zone in the near-wall region. There was only an inert OSW as the main flow structure, as shown in Figure 2(a).

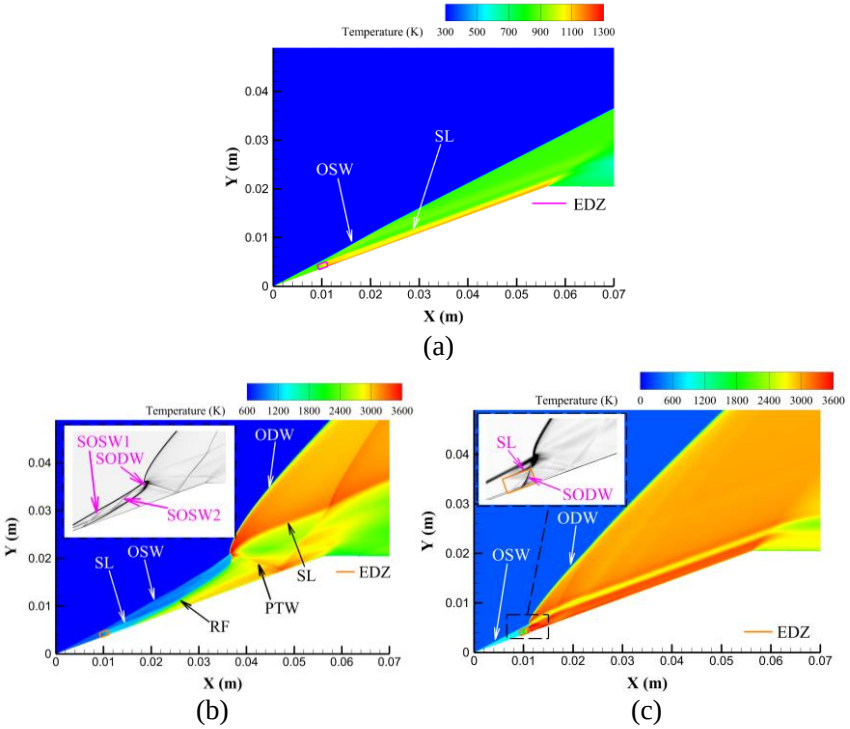

Figure 2: Comparisons of temperature contours with numerical Schlieren zoomed in among different initiation modes under continuous energy deposition, (a) P_{in} = 12 kW/cm, (b) P_{in} = 18 kW/cm, (c) P_{in} = 80 kW/cm.

In contrast, at P_{in} = 18 kW/cm, as shown in Figure 2(b), decoupled combustion occurred downstream of the EDZ, forming a reaction front. The rapid heat release from the reaction front generated a secondary OSW (SOSW1 in Figure 2(b)), which intensified downstream combustion and increased the reaction front angle. Pressure mismatch between regions downstream of the reaction front and slip line produced another secondary OSW (SOSW2 in Figure 2(b)), jointly transitioning combustion into detonation, forming a secondary ODW (SODW in Figure 2(b)). The combustion initiation in this mode was confined exclusively downstream of the EDZ, as was the detonation initiation. Hence, this mode was classified as a Delayed Initiation Mode. As P_{in} = 80 kW/cm, as shown in Figure 2(c), the EDZ generated extremely intensive heating, forming a slip line. The reaction front and the secondary ODW (SODW in Figure 2(c)) could be directly initiated within the EDZ, indicating that the detonation initiation could solely rely on the energy deposition rather than several compressions by secondary OSWs. This initiation mode was classified as the Direct Initiation Mode. Moreover, in this mode, the initiation locations were controllable since the placement of the EDZ was objectively decided by the requirements of practical applications. Thus, adopting high continuous energy deposition power to achieve Direct Initiation Mode was favorable for practical applications.

3.2 Single-pulse Energy Deposition

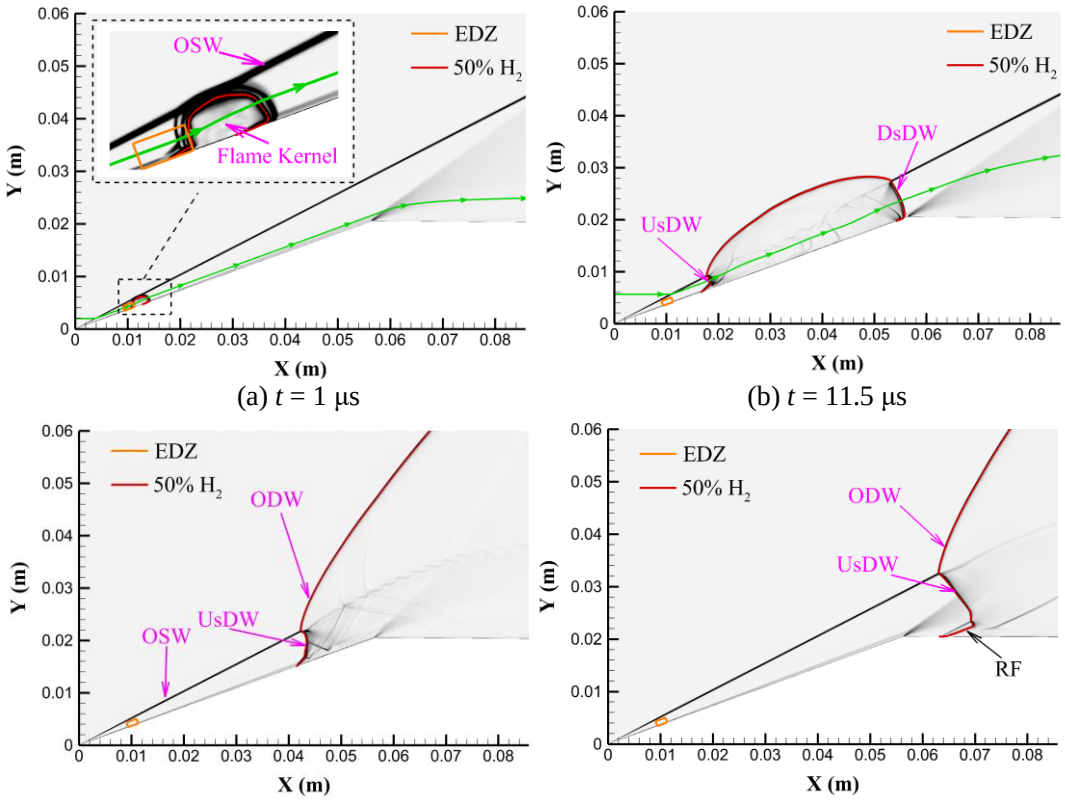

(a) t = 1 μs (b) t = 11.5 μs

(c) t = 81 μs (d) t = 138 μs

Figure 3: Evolution of flow fields of ODW initiation in a typical Direct Explosion-spot Mode under the single-pulse deposition energy E_{sp} of 50 mJ/cm at (a) 1 μs, (b) 11.5 μs, (c) 81 μs, and (d) 138 μs.

The flow field evolution under single-pulse deposition energy E_{sp} = 50 mJ/cm is shown in Figure 3. At t = 1 μs, as shown in Figure 3(a), the pulsatile energy deposition induced combustion within the EDZ. A flame kernel was formed and then gradually propagated downstream. Through this process, the combustion within the reaction front is gradually coupled with shock waves, initiating detonation. The coupled shock wave and the upstream edge of the flame kernel formed the upstream detonation wave (UsDW), whereas the coupled shock wave and the downstream one formed the downstream detonation wave (DsDW). By t = 11.5 μs, as shown in Figure 3(b), the flaming area was significantly expanded by the UsDW and the DsDW. Relative to the incoming flow, the UsDW propagated upstream while the DsDW propagated downstream. Concurrently, both UsDW and DsDW were maintained as detonation waves throughout their propagation. At t = 81 μs, as shown in Figure 3(c), the DsDW had already propagated outside the computational domain, whereas the UsDW was still on the wedge. This implied that the UsDW exhibited a significantly lower propagating speed than the DsDW in the wedge's coordinate system. At t = 138 μs, the UsDW had propagated downstream of the expansion corner. Eventually, it would propagate out of the computational domain, leaving only the OSW as the main flow structure.

3.3 Multi-pulse Energy Deposition

The transient evolution of the main flow structures in multi-pulse energy deposition can be predicted by analyzing the same flow structures under single-pulse energy deposition. Here an assumption can be made based on the single-pulse results: If the UsDW by the n^{th} pulse can be overtaken by (or collide with) the DsDW from the $(n+1)^{th}$ pulse before the expansion corner, as shown in Figure 4(a), and both the distance and the time taken by the collision are short enough, it can be approximated that a sustainable on-wedge detonation has occurred, which to a certain extent is similar to the stable detonation produced by the continuous energy deposition. The length from the wedge tip to the collision

point of DWs for achieving sustainable on-wedge detonation is defined as the equivalent initiation lengths L_{eq}.

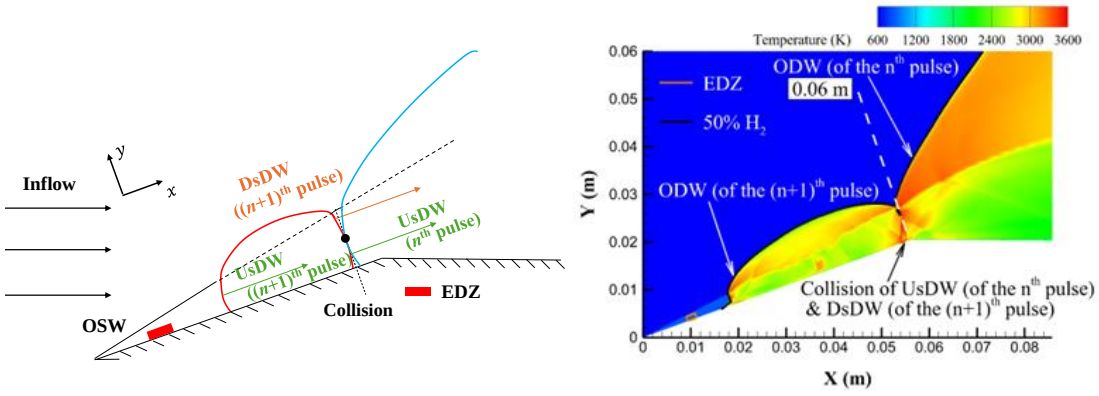

(a) (b)

Figure 4: (a) A schematic of the UsDW generated by the n^{th} pulse chased up by the DsDW generated by the $(n+1)^{th}$ pulse on the finite wedge under multi-pulse energy deposition, (b) The transient flow field as the n^{th} pulse chased up by the DsDW generated by the $(n+1)^{th}$ pulse on the finite wedge under multi-pulse energy deposition with f = 10 kHz.

To achieve the aforementioned sustainable on-wedge detonation under multi-pulse energy deposition, an appropriate pulse repetition frequency, f, must be employed. When f precisely equals the reciprocal of the arrival time interval of detonation waves at the end of the wedge, signifying that the DsDW generated by the $(n+1)^{th}$ pulse collides with the UsDW produced by the n^{th} pulse precisely at the location of the expansion corner. This particular frequency is defined as the critical pulse repetition frequency, f_{cri}, which was found to be 9.15 kHz. A slightly higher f than the f_{cri} was adopted for validation as shown in Figure 4(b).

The condition of E_{sp} = 50 mJ/cm and f = 50 kHz was adopted to achieve a short equivalent initiation length L_{eq} on the wedge. The sustainable on-wedge detonation was achieved, as shown in Figure 5(a). The locations of wave fronts (reaction fronts or ODWs) are shown in Figure 5(b). Within the duration of one pulse, the pulsatile energy deposition achieved rapid initiation of ODW with an equivalent initiation length L_{eq} of only 0.0125 m. It was very close to the downstream edge of the EDZ (0.012 m).

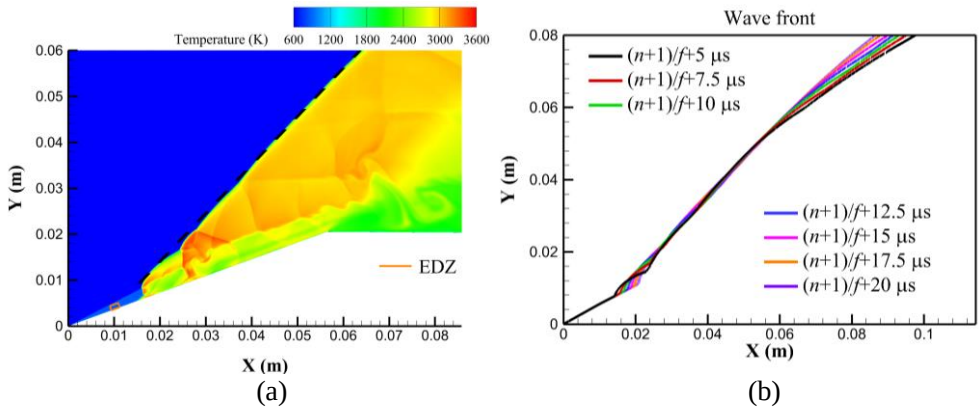

(a) (b)

Figure 5: (a) Temperature contour of sustainable detonation waves on the wedge at t = $(n+1)/f$+7.5 μs, (b) locations of wave fronts under multi-pulse energy deposition at E_{sp} = 50 mJ/cm and f = 50 kHz at different time stamps.

The sustainable detonation could be achieved on the finite wedge by pulsatile energy deposition not only in a very short L_{eq} but also with much less power input P_{in}. Under pulsatile energy deposition, a

similar L_{eq} could be obtained by only using 8.9% of the P_{in} that was used under continuous energy deposition. Therefore, employing pulsatile energy deposition can significantly reduce the power consumption of continuous cases by approximately one order of magnitude, presenting a more widely ranged specification for plasma-generating equipment, which is advantageous for practical engineering applications.

4 Conclusion

This study numerically investigated the feasibility of utilizing a small rectangular EDZ to mimic plasma-induced gas heating effects and assist ODW initiation on the finite wedge. Different initiation modes were observed under continuous energy deposition. Spatiotemporal characteristics of the main flow structures under single-pulse energy deposition were analyzed, enabling the calculation of a minimum pulse repetition frequency required for sustainable detonations on the finite wedge. The multi-pulse energy deposition reduced the energy consumption by over an order of magnitude compared to continuous energy deposition, but maintained similar initiation lengths. This work numerically demonstrated the effectiveness of plasma-assisted initiation methods, providing references to the future design of wide-range ODE combustors.

Acknowledgments

This work was supported by the National Natural Science Foundation of China (Grant Nos. 12202374, Grant Nos. 12472239) and the Hong Kong Research Grants Council (Grant Nos. 15204322).

References

[1] Teng H, Tian C, Zhang Y, Zhou L, and Ng HD. (2021). Morphology of oblique detonation waves in a stoichiometric hydrogen–air mixture. J Fluid Mech 913: A1.
[2] Teng H, Bian J, Zhou L, and Zhang Y. (2021). A numerical investigation of oblique detonation waves in hydrogen-air mixtures at low mach numbers. Int J Hydrog Energy 46: 10984-10994.
[3] Xiang G, Li X, Sun X, and Chen X. (2019). Investigations on oblique detonations induced by a finite wedge in high altitude. Aerosp Sci Technol 95: 105451.
[4] Kimura I, Aoki H, and Kato M. (1981). The use of a plasma jet for flame stabilization and promotion of combustion in supersonic air flows. Combust Flame 42: 297-305.
[5] Ju Y and Sun W. (2015). Plasma assisted combustion: Dynamics and chemistry. Prog Energy Combust Sci 48: 21-83.
[6] Edwards JR and Chandra S. (1996). Comparison of eddy viscosity-transport turbulence models for three-dimensional, shock-separated flowfields. AIAA J 34: 756-763.
[7] Jachimowski CJ. (1988). An analytical study of the hydrogen-air reaction mechanism with application to scramjet combustion. NASA Tech Rep.
[8] Maccormack R. (1990). Modeling supersonic combustion using a fully-implicit numerical method. 26th Joint Propulsion Conference.
[9] Hao J, Wang J, and Lee C. (2016). Numerical study of hypersonic flows over reentry configurations with different chemical nonequilibrium models. Acta Astronaut 126: 1-10.
[10] Hao J and Wen CY. (2020). Hypersonic flow over spherically blunted double cones. J Fluid Mech 896: A26.
[11] Hao J. (2023). On the low-frequency unsteadiness in shock wave–turbulent boundary layer interactions. J Fluid Mech 971: A28.
[12] Van Leer B. (1979). Towards the ultimate conservative difference scheme. V. A second-order sequel to Godunov's method. J Comput Phys 32: 101-136.